Reconfigurable Linear Optical FM Discriminator

Mahmoud S. Rasras, Young-Kai Chen, Kun-Yii Tu, Mark P. Earnshaw, Flavio Pardo, Mark A. Cappuzzo, Evans Y. Chen, Louis T. Gomez, Fred Klemens, Bob Keller, Cristian Bolle, Larry Buhl, John M. Wyrwas, Ming C. Wu, Robert Peach, Scott Meredith, Charles Middleton, and Richard DeSalvo

***Abstract*— We present a reconfigurable optical discriminator filter for frequency modulated microwave-photonics link applications. The filter is based on a simplified ring-assisted Mach–Zehnder interferometer configuration. It enables conversion of a highly linear frequency to amplitude modulation. Operations in a fixed bandwidth (BW) of 30 GHz and a tunable bandwidth from 10 to 30 GHz are achieved using third- and fifth-order filters. A balanced frequency discrimination architecture with electronically reconfigurable transfer characteristics is demonstrated. We measured a ∼7.8 dB output-third order intercept point (OIP3) linearity improvement over that of a dual-output Mach–Zehnder.**

***Index Terms*— Bandpass filter, high-index-contrast waveguide, microwave photonics, optical communications, routing.**

I. Introduction

FREQUENCY modulated (FM) analogue optical fiber links have been shown to provide a promising alternative to intensity modulated (IM) links with a much enhanced dynamic range [1]–[3]. This FM modulated optical signal promises linear transmission of the analog signals with low signal distortion in a low loss optic fiber. To convert the FM modulated optical signal to the linear electrical signal, a linear FM discriminator based on optical field is preferred to attain a high dynamic range [3], where the amplitude frequency response increases with a linear slope from 0 to 1. In a single-ended detection scheme, the photo-detected output of a perfectly linear filter would be distorted significantly by the second-order harmonics through the intensity detection process, but has no third- or higher- order distortions. Using a balanced detection architecture, these second-order harmonics can be effectively cancelled with two discriminators of opposing conversion slopes (see Fig. 1a) [2], [3].

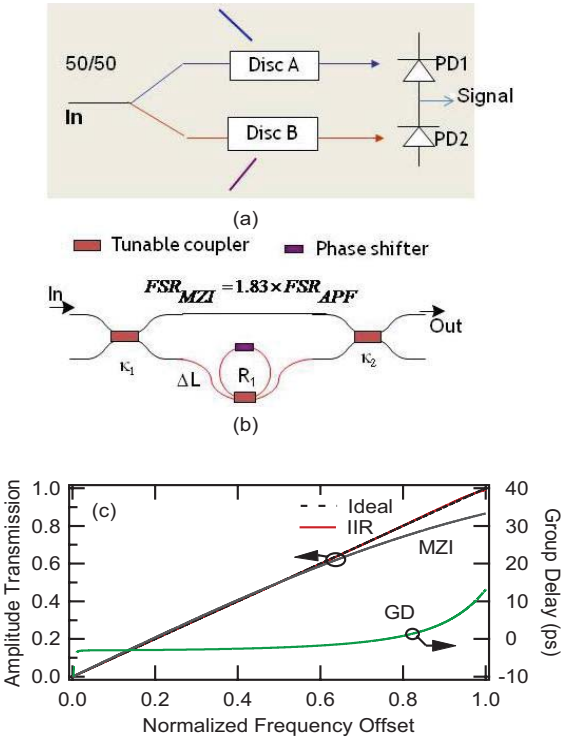

Fig. 1. (a) Balanced optical discriminator layout. (b) Schematic of a third-order (single APF) RAMZI discriminator. (c) Calculated third-order FM discriminator response in comparison to a single stage MZI. Dashed-dotted line: Group delay of the discriminator.

A linear discriminator function can be implemented using a chirped fiber Bragg grating (FBG) [4]. Although it provides excellent transmission linearity, it requires careful fabrication steps to achieve the desired response. A simpler design can be implemented using an imbalanced Mach–Zehnder interferometer (MZI). However, the MZI inherently produces a large third-order harmonic distortion due to the sinusoidal nature of its frequency response. This distortion would limit the dynamic range of the RF link. Recently, linear discriminator filters implemented in a planar lightwave circuit (PLC) were reported by using add-drop ring resonator [5], [6] and cascaded multi-stage MZI finite impulse response filters (FIR) [3], [7]. Additionally, other integrated designs were also proposed based on a ring-assisted MZI (RAMZI) architecture by employing cascaded ring resonators coupled to one of its arms [8]. Nevertheless, the reported designs require a large number of cascaded stages similar to the FIR filter, to achieve a desired linear response. In this letter, we propose a simplified RAMZI linear discriminator architecture with high

Manuscript received May 7, 2012; revised August 22, 2012; accepted September 3, 2012. Date of publication September 6, 2012; date of current version September 26, 2012. This material was based upon work supported by DARPA's TROPHY Program, under AFRL Contract FA8650-10-C-7003. Any opinions, findings, and conclusions or recommendations expressed in this material are those of the authors.

M. S. Rasras, Y.-K. Chen, K.-Y. Tu, M. P. Earnshaw, F. Pardo, M. A. Cappuzzo, E. Y. Chen, L. T. Gomez, F. Klemens, B. Keller, and C. Bolle are with Bell Laboratories, Alcatel-Lucent, Murray Hill, NJ 07974 USA (e-mail: mahmoud.rasras@alcatel-lucent.com).

L. Buhl is with Bell Laboratories, Alcatel-Lucent, Holmdel, NJ 07733 USA.

J. M. Wyrwas and M. C. Wu are with the Department of Electrical Engineering and Computer Sciences, University of California, Berkeley, CA 94720 USA.

R. Peach, S. Meredith, and C. Middleton are with Harris Corporation, Melbourne, FL 32905-0037 USA.

R. DeSalvo is with Bell Laboratories, Alcatel-Lucent, Murray Hill, NJ 07974 USA, and also with Harris Corporation, Melbourne, FL 32905-0037 USA.

Color versions of one or more of the figures in this letter are available online at http://ieeexplore.ieee.org.

Digital Object Identifier 10.1109/LPT.2012.2217483

dynamic range and reconfigurable transfer characteristics for ultra linear response. The proposed design requires only a single stage all-pass filter (APF ring resonator) coupled to the delay arm of a Mach–Zehnder interferometer (see Fig. 1b).

II. Design

The proposed FM discriminator filter is based on a pole-zero filter architecture [8]. It consists of a Mach–Zehnder interferometer (MZI) with a 3-dB splitter at its input and a 3-dB combiner at the MZI output. Either a single or multiple all-pass filters (APFs ring resonators) with a coupled waveguide delay is embedded in each of the MZ arms. A cartoon of the device layout is shown in Fig. 1b.

In an ideal linear FM discriminator filter, the amplitude transfer function satisfies the following equation:

$$h(\omega) = A(\omega - \omega 0)\exp^{(-j\tau(\omega-\omega 0))} \tag{1}$$

where ω is the optical angular frequency, ω_0 is the central frequency, τ is the filter's group delay and $j = \sqrt{-1}$. The proposed transfer function of a RAMZI discriminator with one ring resonator is:

$$h(\omega) = -j\frac{1}{2}\left(1 + \exp^{(-j\tau_{z=mzi}(\omega-\omega 0)-j\varphi_0)} \times \left[\frac{e^{-j\varphi_r}\left(\rho_r e^{+j\varphi_r} - z^{-1}\right)}{1-\rho_r e^{-j\varphi_r} z^{-1}}\right]\right) \tag{2}$$

where $z^{-1} = \exp^{-j\tau_r(\omega)}$, $\rho_r = \sqrt{1-\kappa_r}$, κ_r is the ring coupling ratio, τ_r and τ_{mzi} are the ring and MZI unit delays, respectively. The constants φ_{w} and φ_r are the phases from MZI delay line and ring, respectively. The transfer function of RAMZI can be solved using numerical techniques which is in the form of a transcendental equation. We found that to achieve a transfer function with high linearity, the FSRs of the filter and APF should satisfy the following condition:

$$FSR_{\text{mzi}} = \frac{1}{\tau_{\text{mzi}}} = 4 \times f_{\max}, \quad \text{and} \quad FSR_{APF} = \frac{1}{\tau_r} \cong 2.3 \times f_{\max} \tag{3}$$

where $f_{\max} = BW$ is the maximum modulation frequency at which the discriminator amplitude response equals unity.

An MZI with a single-stage APF is suitable for operations with a fixed FM bandwidth. To achieve operations with adaptive and adjustable bandwidth, a cascaded multi-stage filter is needed. Figure 1c, shows the calculated amplitude transfer function of a single-stage APF RAMZI (3rd order) discriminator. The transfer function of an MZI with similar bandwidth is plotted for comparison. Clearly, a significant improvement in linearity over a simple MZI discriminator is observed by just incorporating a single APF. In addition, this architecture offers a great flexibility in reducing the ripple in the filter's transfer function as it employs a small number of stages coupled to only one of the MZI arms. This further simplifies the tuning algorithm for this device. The impact of the APF finite round trip loss (RTL) on the FM discriminator response and group delay is shown in Fig. 2.

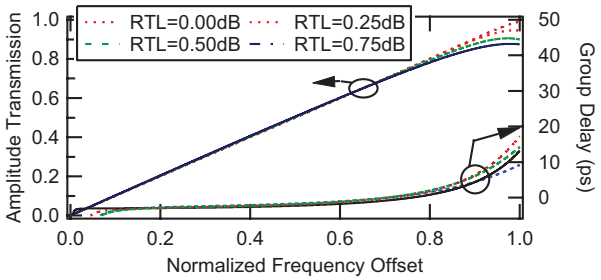

Fig. 2. Impact of the resonator RTL on the discriminator frequency and group delay response.

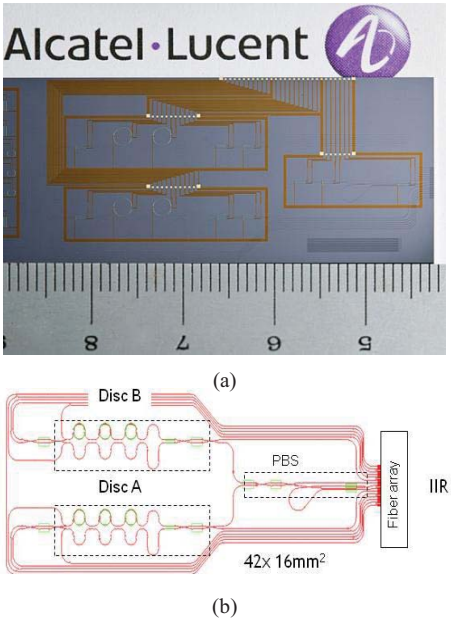

Fig. 3. Layout of a fifth-order RAMZI. (a) Photo. (b) Cartoon.

As the RTL increases, the bandwidth of the discriminator is reduced. Over more than 85% of the bandwidth tuning, the discriminator response remains linear with the modulated FM optical signal, even in the presence of relatively high ring losses (RTL = 0.75 dB). We also observed negligible impact on the calculated group delay response.

III. Experimental Results

The balanced optical discriminator has been fabricated in a high-index-contrast (HIC) 4% silica-on-silicon planar lightwave circuit (PLC) with a relatively compact footprint of 4.5 cm × 2 cm. In this device, a single-mode waveguide dimension of 2.2 μm × 2.7 μm is used. A lower and upper cladding thickness of 15 μm and 6 μm, respectively, are deposited around the waveguide for optical isolation. For a compact design, a minimum bend radius of 350 μm is implemented throughout the device which introduces negligible bend losses. The propagation loss of a single-mode waveguide is 0.045 dB/cm. A Photo and a cartoon of the layout of the 5th order design are shown in Fig. 3. Thermo-optic phase shifters are used to tune the filter coefficients.

The optical path in balanced discriminator chip is described below. The input FM-optical signal enters the chip at the right

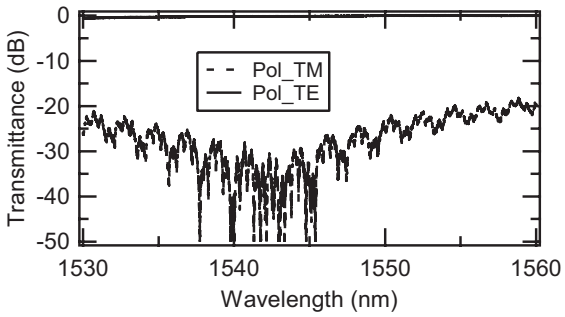

Fig. 4. Measured PBS transmittance at TE output port.

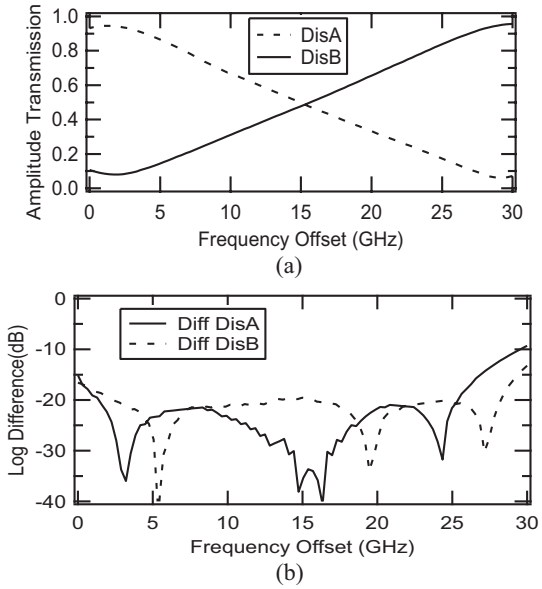

Fig. 5. (a) Measured transfer function of a tunable balanced discriminator. DisA and DisB are tuned to positive and negative slopes. (b) Logarithmic base 10 difference between measured and ideal discriminator curves.

hand-side of Figure 3 is first coupled into a polarization beam splitter (PBS). The PBS ensures that the balanced discriminator filters receive either a pure TE or TM signal. The measured wavelength response of the PBS is shown in Fig. 4. The PBS assures a high polarization splitting extinction ratio over a broad wavelength range. The separated TE or TM signals from the PBS are then coupled to the balanced discriminators which are optimized for either TE or TM operation. The discriminators convert the FM signal into amplitude modulated signals which are then coupled via fiber array to off-chip balanced photodiodes.

Two optical discriminator designs were explored; the first one is a 3rd order filter designed to achieve a fixed BW = 30 GHz. And the second is a 5th order filter suitable for reconfigurable BWs from 10 to 30 GHz. Both designs are integrated with APF FSRs of 69 GHz while the MZI FSR is 120 GHz. Figure 5a demonstrates the measured transfer function of a balanced 3rd order discriminator chip with the transfer functions of the discriminators set to have opposite slopes. The crossing point of the two curves is set at 50% of the amplitude value in this case but can be further adjusted to optimize the RF link performance. Fig. 5b shows the

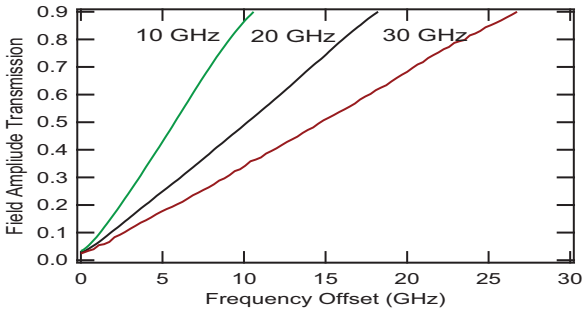

Fig. 6. Measured transfer function of a tunable fifth-order RAMZI discriminator set to achieve BW between 10 and 30 GHz.

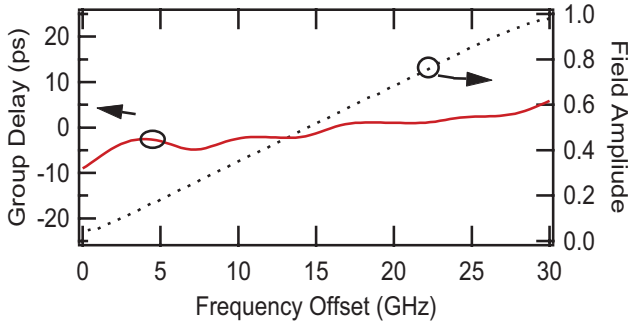

Fig. 7. Measured group delay response of a tunable discriminator where BW is set at 30 GHz.

difference between the measured discriminators responses and the calculated ideal responses for both the negative and positive slopes. We observed excellent agreement between the simulated and measured curves. The deviations from ideal performance is due to finite APF losses (measured RTL = 0.1 dB) and to slight inaccuracies in the RAMZI filter coefficient tuning.

To demonstrate the ability to tune the discrimination bandwidth, we employed the 5th order filter to achieve adjustable BWs of 10, 20 and 30 GHz. The measured frequency transfer functions are shown in Fig. 6, the curves demonstrate highly linear response for different bandwidths, verifying the high adjustability of this design. The measured 5th order filter's group delay (GD) response is depicted in Fig. 7, shown for the filter set at 30 GHz bandwidth. The group delay response exhibits small variations across the measured BW; further reducing distortion in the RF link [3].

Note that, for both filter types, the chip insertion loss is ~7 dB, which includes 2.5 dB fiber coupling loss, 3 dB power splitting between the two discriminators, and 1.5 dB from the intrinsic loss of the various components of the discriminator chip (including PBS, splitters and couplers).

Fig. 8 shows a diagram of a phase modulated microwave photonic link setup discriminated with balanced optical IIR filters. Two radio frequency synthesizers are used to generate tones at f and $f + 0.0001$ GHz with equal RF powers, and they are combined with a microwave coupler. Light from an external cavity laser is modulated with a lithium niobate phase modulator. The light is passed through the balanced tunable filters and photodetected, then the signal is viewed on an

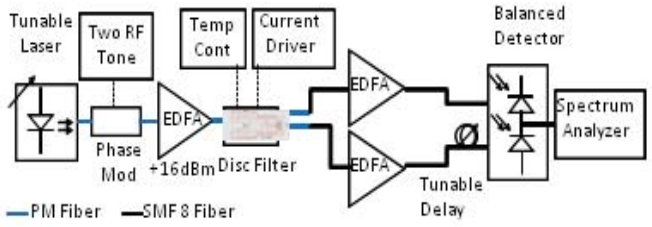

Fig. 8. Diagram of phase-modulated microwave photonic link.

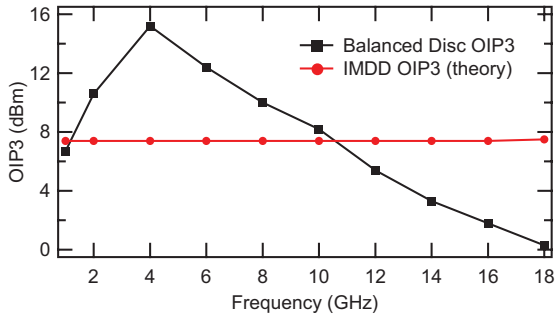

Fig. 9. OIP3 for a balanced 30 GHz discriminator link. The total photocurrent at the detector is kept constant at 10.5 mA.

electrical spectrum analyzer. The optical power is amplified so that the total DC is constant. The photodetector impedance (Zout) is 12.5 Ohm,

Fig. 9 illustrates the measurement of link response versus modulation frequency for a 30 GHz balanced discriminator vs intensity modulation direct detection (IMDD) link. We assume IMDD link employs a dual output Mach–Zehnder modulator (MZM) biased at quadrature point [10]. As shown in this figure, the FM-DD link demonstrates an optimal ratio of fundamental to third-order intermodulation distortion (IMD3) power at 1549.964 nm carrier wavelength. This operating wavelength corresponded with a point where the filter has 50% amplitude transmission. During testing, the wavelength is kept stable to within $+/-2$ pm of set-point. For a photocurrent of 10.5 mA, added from the two balanced photodetectors, the measurements shows that the discriminator output-third order intercept point (OIP3) exceeds equivalent IMDD from 1–11 GHz.

Fig. 10 depicts the measurement of link response versus modulation power measured at an optimal RF frequency around 4 GHz (total photodetector current = 10.5 mA). The equivalent IMD3 from a dual Mach Zehnder interferometer (MZI) is plotted on the same figure (squares). We measured an OIP3 of 15.2 dBm which gives a 7.8 dB OIP3 improvement over a MZI with the same received photocurrent. Note that, the OIP3 for an IMDD link ($OIP3_{IMDD}$) is equal to $4I_{dc}^2 Z_{out}$ [10], where I_{dc} is the photocurrent summed from both of the balanced detectors. Therefore, the calculated $OIP3_{IMDD}$ is equal to 7.4 dBm.

Furthermore, because the discriminator FM receiver is a balanced device, the second-order distortion is also low over the whole band.

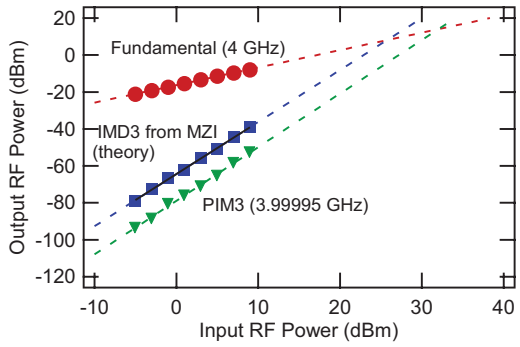

Fig. 10. Measurement of link response versus modulation power for a balanced 30 GHz. The photocurrent is fixed at 10.5 mA and the wavelength is fixed at 1549.964 nm.

IV. Summary

We have demonstrated a balanced optical discriminator filter with excellent linearity in field amplitude frequency response. The filter is based on a RAMZI architecture which only requires a small number of APF stages and can provide both fixed and adjustable FM bandwidth. We demonstrated good linearity for a low-frequency FM-DD link. We expect that using such discriminators together with balanced photodetectors can significantly increase the signal gain and achieve low second-harmonic distortion [3]. Furthermore, this type of electronically reconfigurable FM discriminator can potentially offer distinctive advantages in providing adaptive compensation and equalization of an FM modulated signal to mitigate non-ideal component characteristics; for example, equalization of the nonlinear FM laser response.

References

[1] W. Sorin, K. Chang, G. Conrad, and P. Hernday, "Frequency domain analysis of an optical FM discriminator," *J. Lightw. Technol.*, vol. 10, no. 6, pp. 787–793, Jun. 1992.

[2] T. E. Darcie, J. Zhang, F. Driessen, and J.-J. Eun, "Class-B microwave-photonic link using optical frequency modulation and linear frequency discriminators," *J. Lightw. Technol.*, vol. 25, no. 1, pp. 157–164. Jan. 2007.

[3] J. M. Wyrwas and M. C. Wu, "Dynamic range of frequency modulated direct-detection analog fiber optic links," *J. Lightw. Technol.*, vol. 27, no. 24, pp. 5552–5561. Dec. 15, 2009.

[4] J. C. Chen and R. A. Brown, "Novel optical frequency discriminator with 'perfect' linearity," in *Proc. OFC 2000 Conf.*, p. 329, paper WM40-1.

[5] D. A. I. Marpaung, C. G. H. Roeloffzen, R. B. Timens, A. Leinse, and M. Hoekman, "Design and realization of an integrated optical frequency modulation discriminator for a high performance microwave photonic link," in *Proc. IEEE MWP 2010*, Oct., pp. 131–134.

[6] D. Marpaung, C. Roeloffzen, A. Leinse, and M. Hoekman, "A photonic chip based frequency discriminator for a high performance microwave photonic link," *Opt. Express*, vol. 18, no. 26, pp. 27359–27370, 2010.

[7] J. M. Wyrwas, *et al.*, "Dynamic linearity improvement of phase and frequency modulated microwave photonic links using optical lattice filter discriminators," in *Proc. IEEE MWP 2011*, Oct., pp. 41–44.

[8] X. Xie, J. Khurgin, J. Kang, and F. Choa, "Ring-assisted frequency discriminator with improved linearity," *IEEE Photon. Technol. Lett.*, vol. 14, no. 8, pp. 1136–1138, Aug. 2002.

[9] M. S. Rasras, *et al.*, "Demonstration of a fourth-order pole-zero optical filter integrated using CMOS processes," *J. Lightw. Technol.*, vol. 25, no. 1, pp. 87–92, Jan. 2007.

[10] V. J. Urick, F. Bucholtz, P. S. Devgan, J. D. McKinney, and K. J. Williams, "Phase modulation with interferometric detection as an alternative to intensity modulation with direct detection for analog-photonic links," *IEEE Trans. Microw. Theory Tech.*, vol. 55, no. 9, pp. 1978–1985, Sep. 2007.